Instrument Science Report STIS 2016-01(v1)

Determination of the STIS CCD Gain

Allyssa Riley[1], TalaWanda Monroe[1], Sean Lockwood[1]

[1] Space Telescope Science Institute, Baltimore, MD

29 September 2016

ABSTRACT

This report summarizes the analysis and absolute gain results of the STIS Cycle 23 special calibration program 14424 that was designed to measure the gain of amplifiers A, C and D at nominal gain settings of 1 and 4 e^-/DN. We used the mean-variance technique and the results indicate a $< 3.5\%$ change in the gain for amplifier D from when it was originally calculated pre-flight. The gain measurements for a nominal gain setting of 1 were 1.028, 0.991 and 1.034 e^-/DN for amps A, C and D, respectively. For a nominal gain setting of 4 e^-/DN, they were measured to be 3.993, 4.100 and 4.087 e^-/DN, respectively. We compared these values to previous measurements from Cycles 17 through 23. This report outlines the observations, methodology, and results of the mean-variance technique.

Contents

Operated by the Association of Universities for Research in Astronomy, Inc., for the National Aeronautics and Space Administration.

1. Introduction

The Space Telescope Imaging Spectrograph (STIS) was installed on the Hubble Space Telescope (HST) in 1997. One of its detectors is a 1024x1024 square pixel CCD with $\sim$0.05"x0.05" pixels and a field of view of 52"x52" (Biretta, 2016). When photons hit a pixel on a CCD, electrons are liberated via the photoelectric effect. The gain quantifies the number of liberated electrons recorded before the detector counts them as a single Data Number (DN). It is important to know the value of the gain because it is propagated through the CalSTIS pipeline and provides a way to diagnose any changes in the electronics of the detector. The measured gain is also used in analyzing the charge transfer inefficiency (CTI).

A special calibration program was designed to redetermine the gain values for amplifiers A, C, and D, at nominal gain settings of 1 and 4 e^-/DN. This report outlines the observations, methodology, and results, and compares the results to measurements from the STIS CCD General Performance Monitor from previous years.

2. Theory

To calculate the gain, we use the mean-variance technique. The primary assumption of the mean-variance technique is that the total noise is comprised of only the read noise and the photon noise. When Poisson noise sources are independent of each other, they may be added in quadrature, such that the total noise, N, may be written as

$$\left(\frac{N}{g}\right)^2 = \left(\frac{P}{g}\right)^2 + \left(\frac{RN}{g}\right)^2, \tag{1}$$

where P is the photon noise, RN is the read noise and g is the gain. The photon noise obeys Poisson statistics and is related to the mean signal by $P = \sqrt{\mu g}$. The total noise term, or observed variance in an image σ^2, can thus be written as

$$\sigma^2 = \frac{\mu}{g} + \left(\frac{RN}{g}\right)^2. \tag{2}$$

Equation 2 shows a linear relationship between the variance, σ^2, and the mean signal, μ, where the slope is $1/g$, or the inverse of the gain (Gosmeyer & Baggett, 2015).

3. Observations

The observations for Cycle 23 special program 14424 (PI: John Biretta) consist of 6 pairs of internal tungsten flat fields at exposure times ranging from 0.1 to 100 seconds for amplifiers A, C and D, and at nominal gain settings of 1 and 4 e^-/DN, resulting in a total of 72 single flat frames. The neutral density filter F25ND3 was used so that the pixels would not reach saturation even at the longest exposure times. This resulted in a count range of $\sim$100 - 17,000 DN, over the range of the exposure times. The F25ND3

filter covers the middle 25”x25” of the CCD. This allows only the center quarter of the CCD to be illuminated. All observations were made on 26 October 2015, 3.5 weeks after an anneal, to minimize the effects of the anneal on the CCD properties. The observations are detailed in Table 1.

Table 1.: The list of datasets used in this program along with the amplifiers and gains used as well as the exposure times and the number of exposures.

Filename	Amplifier	Gain (e^-/DN)	Exposure Time (s)	Exposures
od1f01010	D	1	0.1	2
od1f01020	D	1	0.3	2
od1f01030	D	1	1	2
od1f01040	D	1	3	2
od1f01050	D	1	10	2
od1f01060	D	1	30	2
od1f02010	D	4	0.3	2
od1f02020	D	4	1	2
od1f02030	D	4	3	2
od1f02040	D	4	10	2
od1f02050	D	4	30	2
od1f02060	D	4	100	2
od1f03010	A	1	0.1	2
od1f03020	A	1	0.3	2
od1f03030	A	1	1	2
od1f03040	A	1	3	2
od1f03050	A	1	10	2
od1f03060	A	1	30	2
od1f04010	A	4	0.3	2
od1f04020	A	4	1	2
od1f04030	A	4	3	2
od1f04040	A	4	10	2
od1f04050	A	4	30	2
od1f04060	A	4	100	2
od1f05010	C	1	0.1	2
od1f05020	C	1	0.3	2
od1f05030	C	1	1	2
od1f05040	C	1	3	2
od1f05050	C	1	10	2
od1f05060	C	1	30	2
od1f06010	C	4	0.3	2
od1f06020	C	4	1	2
od1f06030	C	4	3	2
od1f06040	C	4	10	2
od1f06050	C	4	20	2
od1f06060	C	4	100	2

Because the STIS CCD shows a coherent herringbone-like read noise pattern, we corrected for it using `batch_run_autofilet.py`, a python interface that calls the IDL script `autofilet.pro` version 1.2 (Jansen, 2015 and Bostroem, 2013). We made minor changes to `batch_run_autofilet.py` so that it would run correctly on the STIS data. We also used code developed specifically to create STIS reference files called `refstis` (Ely, 2013). To run the herringbone correction on the flats, we followed the steps below:

1. Run the raw darks, flats, and biases through `batch_run_autofilet.py`.
2. Run the bias frames from step 1 through the first two steps of CalSTIS by setting `DQICORR` and `BLEVCORR` to `PERFORM` and everything else to `OMIT`.
3. Make the superbias using the herringbone-corrected and `BLEVCORR`-corrected bias frames from step 2 using the `basejoint` function in the `refstis` package.
4. Run the dark frames from step 1 through the first three steps of CalSTIS by setting `DQICORR`, `BLEVCORR`, and `BIASCORR` to `PERFORM` and everything else to `OMIT`. Set `BIASFILE` to point to the herringbone-corrected superbias from step 3.
5. Use the herringbone- and bias-corrected dark frames from step 4 to make a superdark using the `basedark` function in the `refstis` package.
6. Run the flat frames through CalSTIS by setting `DQICORR`, `BLEVCORR`, `BIASCORR`, `CRCORR`, `EXPSCORR` and `DARKCORR` to `PERFORM` in the headers of the flat frames and set `BIASFILE` and `DARKFILE` to point to the herringbone-corrected superbias and superdark from steps 3 and 5, respectively.

Additionally, setting `CRCORR` and `EXPSCORR` flags cosmic rays and hot pixels in individual frames.

4. Method

4.1 Mean-Variance Method

Each pair of calibrated flats were subtracted to produce a difference image and averaged to make a mean image at each exposure time and gain setting. We then divided the illuminated portion of the CCD into 25 overlapping 200x200 pixel regions and eliminated all pixels with data quality flags not equal to zero in either flat. For each region in the average and difference images, we made a histogram of the pixel values and fit a Gaussian to the histogram. We used the mean of the Gaussian from the regions in the average image and the standard deviation of the Gaussian from the regions in the difference image

(σ_{diff}). The variance is $\sigma^2_{diff}/2$. The Gaussian distribution of the pixel values allowed us to implement Scott's rule (Scott 1979) to determine an appropriate histogram bin width. Also, because the distributions of pixel values were well-represented by Gaussians, the uncertainties from the Gaussian fits were small and were used as weights for the linear fits described below. More specifically, the weights were calculated to be the inverse of the diagonal elements of the covariance matrix that was output by the Gaussian fit.

After the mean and variance of all 25 regions for a single pair of flats were found, we used 3-sigma clipping on the variance and eliminated all data points where the mean signal was greater than 30,000 DN in an effort to avoid the nonlinear effects of saturation. Finally, we used the python polynomial fitter `numpy.polyfit` to run a weighted linear fit to the points. The gain is the inverse of the fitted slope.

To calculate the uncertainty in the gain, we used the formal error propagation formula,

$$\frac{\delta_g}{g} = \frac{\delta_m}{m}, \tag{3}$$

where m is the fitted slope and δ_m is the uncertainty in the fitted slope. Because $g = 1/m$, it can be simplified to

$$\delta_g = \frac{\delta_m}{m^2}. \tag{4}$$

The script used to make these calculations can be found in the STIS monitors Grit repository on `grit.stsci.edu`.

4.2 The Monitors Method

The gain of the STIS CCD is measured yearly as part of the General Performance Monitor (i.e. program IDs 14411, 13979, 13534, 13130, 12740, 12396, and 11843) using a simpler, less rigorous method than the mean-variance method that produces larger uncertainties (see Figure 3). It requires only two raw flat frames of the same exposure time and two raw bias frames. In this method, the two flats are subtracted from each other and the two biases are subtracted from each other. The gain is given as

$$g = \frac{\text{mean}(flat_1) + \text{mean}(flat_2) - \text{mean}(bias_1) - \text{mean}(bias_2)}{\sigma^2_{diff\_flat} - \sigma^2_{diff\_bias}} \tag{5}$$

where $flat_1$ and $flat_2$ are the two flats, $bias_1$ and $bias_2$ are the two biases, and $\sigma^2_{diff\_flat}$ and $\sigma^2_{diff\_bias}$ are the variances of the difference flat and the difference bias, respectively (Goudfrooij, 1998).

Although this is a less rigorous method of measuring the CCD gain, we compared the results of the mean-variance technique with the results from equation 5, using the data from the special program for both techniques, to help quantify any discrepancy in the results. These results can be found in section 5.

4.3 The Flux Ratio Method

After SM4, when operations to STIS' side-2 electronics were restored, the gain was measured using a third method (Goodfrooij, et al 2009). By taking observations at two different gain settings (gain = 1 and gain = 4, in this case) we can take the ratio of the fluxes to find the gain:

$$\frac{flux_a}{flux_b} = \frac{gain_b}{gain_a} \tag{6}$$

where flux$_a$ and flux$_b$ correspond to the flux from a standard star or line lamps at gain$_a$ and gain$_b$, respectively. This method requires prior knowledge of one of the gain values so the values calculated using this method has uncertainties associated with the calculation itself as well as the assumption of one of the gain values.

To test this method and compare it to the mean-variance technique, we used data from the STIS CCD Sparse Field CTE program, which takes internal observations of the tungsten lamp, read out using amplifiers A and C and at gain settings 1 and 4 e^-/DN. After measuring the flux of the lamp for each amplifier, we took the ratio of the gain=1/gain=4 fluxes. To compare these values to the mean-variance results, for amplifiers A and C, we divided the calculated gain = 4 value by the calculated gain = 1 value. These results are presented in section 5.

5. Results and Conclusions

Histograms of the pixel values in the average and difference images were plotted to ensure that they were in fact Gaussian distributions. Histograms were made for the 25 regions in each set of images with matching exposure times. We have included representative histograms of average and difference images in Figure 1.

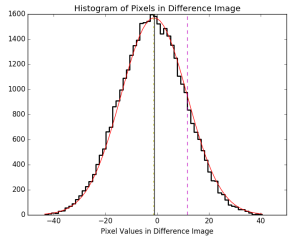

(a) An example of a histogram of the pixel values in one 200x200 pixel region in one difference image.

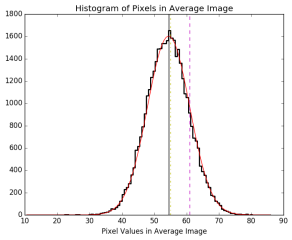

(b) An example of a histogram of the pixel values in one 200x200 pixel region in one average image.

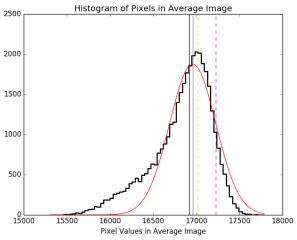

(c) An example of the pixel values in a region in an average image. As exposure time increases, the number of skewed histograms increases.

Figure 1.: Example histograms of the pixel values in the average and difference images. The red line is the fitted Gaussian and the solid gray line indicates the mean of the distribution, as fit by the Gaussian. The dashed magenta line is one standard deviation from the mean, as fit by the Gaussian and the yellow dot-dashed line indicates the peak bin value. The red vertical line is the center of the analytic Gaussian and finally, the vertical black line shows the median value.

Histograms such as the one shown in Figure 1c occur exclusively for the average images at longer exposure times. For the longest exposure times, skewed distributions can occur up to $\sim 60\%$ of the time. We suspect this is due in part to the presence of dust particles seen on the flat fields and also the uneven illumination across the frame. Thus, using the mean of the histogram is not always the best statistical value to use. We assessed how using the mode affected the gain calculations; the discrepancy between the gains calculated using the means and that using the modes of the distribution is $< 0.30\%$. Because the gain was not significantly affected by this change, we adopted the mean for our analysis.

The mean-variance plots for all modes are shown in Figure 2 and gain measurements resulting from these plots are presented in Table 2.

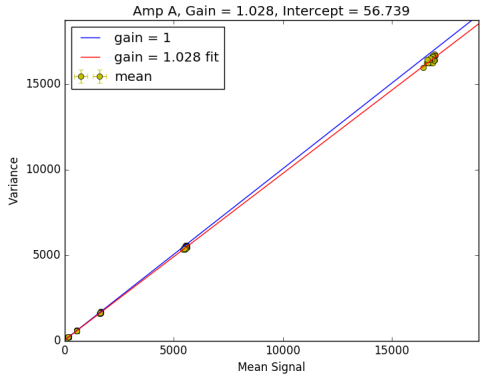

(a) Amplifier A at a nominal gain of 1 e^-/DN

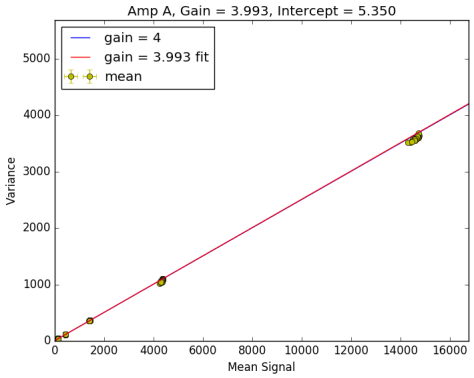

(b) Amplifier A at a nominal gain of 4 e^-/DN

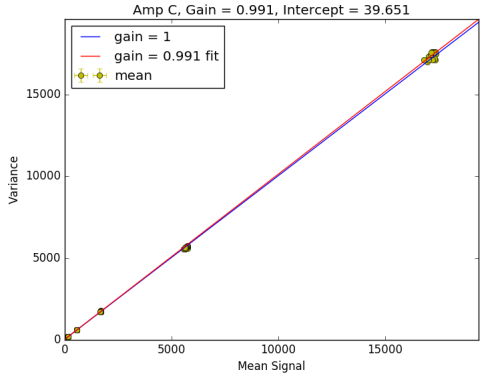

(c) Amplifier C at a nominal gain of 1 e^-/DN

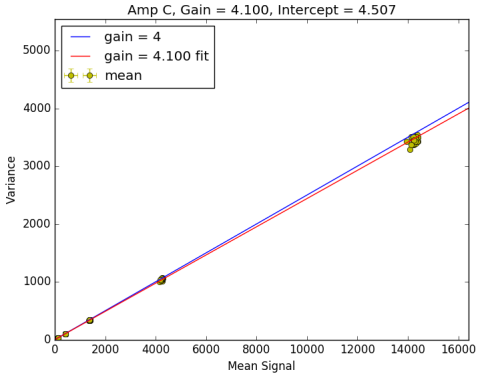

(d) Amplifier C at a nominal gain of 4 e^-/DN

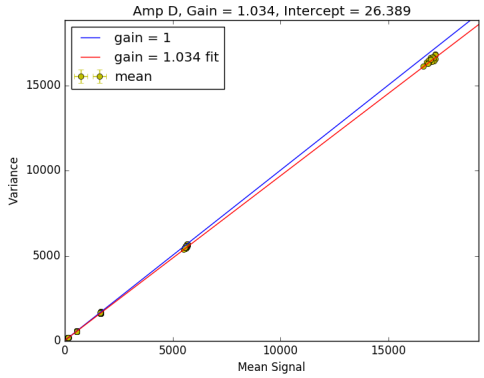

(e) Amplifier D at a nominal gain of 1 e^-/DN

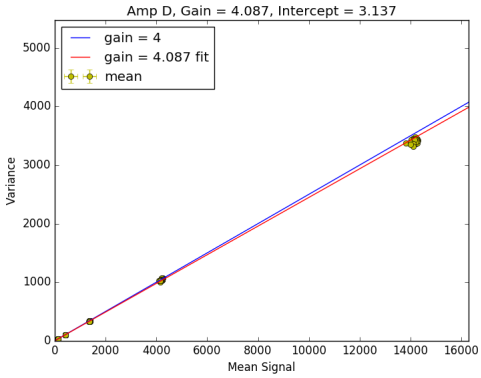

(f) Amplifier D at a nominal gain of 4 e^-/DN

Figure 2.: Mean-variance plots for all amplifiers at each nominal gain. The red line signifies the fitted line, the slope of which is the inverse of the gain for that mode. The blue line shows the nominal gain setting value.

The gain values for amplifier D used in the CalSTIS pipeline are 1.000 and 4.016 e^-/DN, which were calculated in 2009, after Servicing Mission 4 (SM4), when operations to the side 2 electronics were restored (Goodfrooij, et al., 2009). Nominal gain

values of 1.000 and 4.016 e^-/DN were used in calculating the percent discrepancy for amplifier D, as reported in Table 2. Because amplifiers A and C are not monitored as closely, nominal gains of 1.0 and 4.0 e^-/DN are used in the percent discrepancies for amplifiers A and C.

Table 2.: The measured gain values, according to the mean-variance technique per mode, as well as the percent discrepancies between the measured and nominal gains.

Amplifier	Nominal Gain (e^-/DN)	Measured Gain (e^-/DN)	Percent Discrepancy
A	1	1.028 ± 0.001	2.80
A	4	3.993 ± 0.007	0.18
C	1	0.991 ± 0.001	0.90
C	4	4.100 ± 0.007	2.50
D	1	1.034 ± 0.003	3.40
D	4	4.087 ± 0.007	1.77

To provide context for the percent discrepancies reported in Table 2, we have plotted the percent discrepancies of amplifier D, using a nominal gain of 1.000 and 4.016 e^-/DN and the values from the General Performance Monitors between March 2009 and March 2016. It should be noted that in Figure 3a, there are two low data points, where the gain was calculated to be 0.7 e^-/DN and 0.69 e^-/DN. Upon inspection, we found that the monitors method is highly susceptible to cosmic rays and these points were contaminated. Given just cause, we rejected these outliers when computing the standard deviation of the measured gains. We also rejected the two low points in Figure 3b.

We suspect that the rest of the points in Figure 3b are offset from the 0% difference line due to the method used to determine gain = 4.016 e^-/DN (see section 4.3). Goodfrooij, et al (2009) took the gain=4/gain=1 ratio of a standard star assuming the gain=1 setting remained the same value as pre-flight measurements, 1.000 e^-/DN. The final uncertainty in the gain measurement from 2009 is comprised of uncertainties from the measurement but also an additional systematic uncertainty from the original pre-flight gain measurement.

Because data for amplifiers A and C are sparse, we are unable to plot the calculated gain vs. time for them.

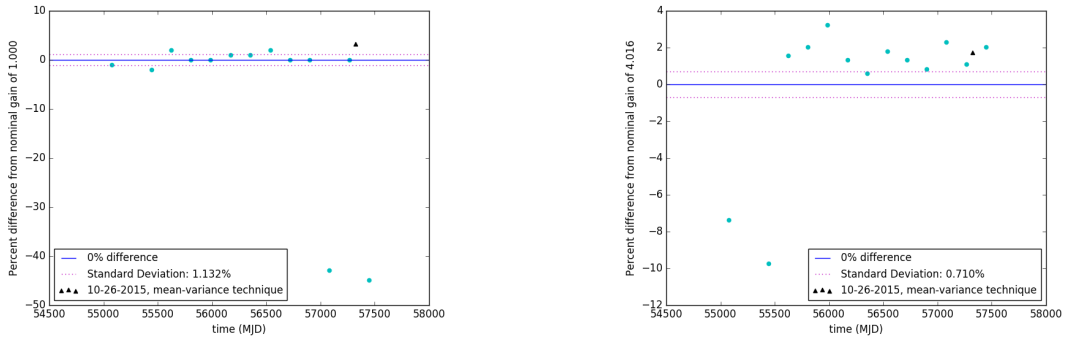

(a) Gain = 1

(b) Gain = 4

Figure 3.: The percent discrepancies in amplifier D compared to gains 1.000 and 4.016 e^-/DN, using the results of the STIS General Performance Monitors from March 2009 through March 2016. The solid blue lines indicate where the results agree with the nominal gain values that are used in the STIS pipeline. The dotted magenta lines indicate where one standard deviation of the data lies. Finally, the black triangles indicate where on the plot the gain calculated with the mean-variance technique for the special calibration program 14424 lie.

Figure 4 shows the results from using the flux ratio method from cycles 17 through 22. There appears to be an offset between the gain ratio using the values calculated with the mean-variance method and the flux ratios calculated using the Sparse Field CTE calibration program. This discrepancy is $< 1.8\%$ and $< 3.4\%$ for the amplifier A and C data, respectively.

Figure 4 does not include error bars on the points because we have not yet been able to characterize the uncertainties in the Sparse Field measurements. We believe they are dominated by systematics, such as lamp brightness variability, rather than Poisson noise. Work on determining the uncertainties in the flux measurements of the Sparse Field data will be done in the future.

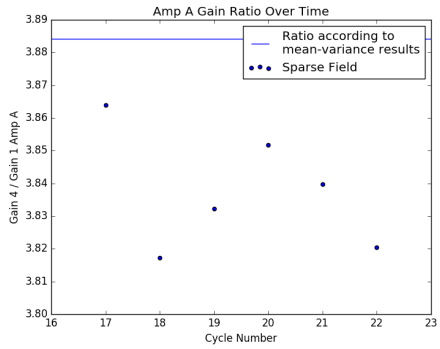

(a) Amplifier A flux ratio

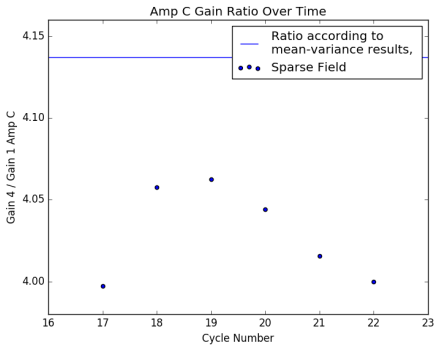

(b) Amplifier C flux ratio

Figure 4.: The results of the flux ratio method using flux values obtained from the internal tungsten lamp. The blue line indicates the ratio of gain = 4/gain = 1 values calculated using the mean-variance technique. The blue points indicate the flux ratio for a given cycle using the sparse field CTE calibration program.

The mean-variance technique is more rigorous than the method used in the monitors described in section 4.2. For one, unlike the mean-variance technique the second method uses calibrated bias frames, which includes cosmic ray rejection. The mean-variance technique also uses more data to make the measurement than the monitors method. Upon further inspection of the STIS CCD General Performance monitor, we found that the gain calculation script contained multiple issues (e.g. not using all available observations, combining observations with different exposure times). However, because the gain values found using the mean-variance technique agree to within a few percent of those reported by the STIS CCD General Performance monitor, these issues may not have a large effect on the gain measurements. These issues with the gain monitor will be investigated more thoroughly in the future. However, with the technique and scripts being used currently, the gain has remained constant to within $\sim 1\%$ for both gain settings 1 and 4 and amplifier D since SM4. This consistency indicates that the STIS CCD is stable.

Like the mean-variance technique, the flux ratio method requires more data than the monitors method. However, the flux ratio method is unique to the other methods because each gain measurement is not independent of the others.

For this project, we investigated the gain of the STIS CCD using the three methods employed over the history of STIS. Each one has biases and systematics unique to the method. However, because our results agree across the three methods to within a few percent, we recommend the continued use of the existing gain values in the pipeline as determined post-SM4, 1.000 e^-/DN and 4.016 e^-/DN for the nominal gain = 1 and gain = 4 settings, respectively for amplifier D and 1 e^-/Dn and 4e^-/DN for amplifiers A and C.

Acknowledgements

We thank Sylvia Baggett for her insight and sharing her understanding of CCDs. We would also like to thank Charles Proffitt and John Debes for their helpful discussion and feedback throughout this process.

References

Biretta, J., et al. 2016, "STIS Instrument Handbook," Version 15.0, (Baltimore: STScI).
Bostroem, A. 2013, "Herringbone Correction." GitHub Repository, `https://github.com/abostroem/science_programs/tree/master/programs/herringbone_correction`
Ely, J. 2013, "refstis." GitHub Repository, `https://github.com/spacetelescope/refstis`
Gosmeyer, C. M. and Baggett, S. 2015, "WFC3 IR Gain from 2010 to 2015." WFC3 ISR 2015-14.
Goudfrooij, P. 1998, "STIS CCD Performance Monitor: Read Noise, Gain, and Consistency of Bias correction during June 1997-June 1998." STIS ISR 98-31
Goudfrooij, P., Wolfe, M.A., Bohlin, R.C., Proffitt, C.R., Lennon, D.J. 2009, "STIS CCD Performance After SM4: Read Noise, Dark Current, Hot Pixel Annealing, CTE, Gain, and Spectroscopic Sensitivity." STIS ISR 2009-02
Jansen, R. 2015, "AR11258 - STIS CCD Side-2 pattern noise removal." `http://stis2.sese.asu.edu`
Scott, David W. (1979). On Optimal and Data-Based Histograms. *Biometrika*, 66(3), 605-610. doi: 10.2307/2335182.